Exchange and hyperfine interactions in Ag:Mn dilute alloys*

D. Davidov†
Racah Institute of Physics, Hebrew University of Jerusalem, Jerusalem, Israel

C. Rettori,‡ R. Orbach,§ A. Dixon, and E. P. Chock
Physics Department, University of California, Los Angeles, California 90024

(Received 20 June 1974)

The electron-spin resonance of dilute Ag:Mn alloys is reported for samples containing Sb and Au nonmagnetic impurities. The bottleneck is nearly broken, allowing for the extraction of the unbottlenecked g value and linewidth. These quantities, together with the Kondo $\ln T$ coefficient as measured by Jha and Jericho, are sufficient to determine the first three partial-wave exchange amplitudes. The three partial-wave amplitudes combine to give a value for the exchange Ruderman-Kittel-Kasuya-Yosida broadening of the host NMR which is only 25% smaller than that measured by Mizuno, and reanalyzed by Alloul. The d-wave amplitude is negative, and smaller in magnitude than in Cu:Mn, implying a very much lower Kondo condensation temperature for Ag:Mn as compared to Cu:Mn. The magnitude of the shift of the ^{55}Mn hyperfine field in Ag:Mn from the insulating state is shown to be consistent with these exchange partial-wave amplitudes. The conduction-electron spin-flip relaxation rate is extracted for each of the two impurities, Sb and Au. Finally, a line-shape analysis taking into account exchange narrowing of the hyperfine splitting is shown to partially explain the concentration dependence of the "residual width" in reflection ESR, consistent with the behavior of $1/T_{dL}$ in transmission ESR.

I. INTRODUCTION

The electron-spin resonance (ESR) of Ag:Mn and Cu:Mn has been extensively studied by many authors[1-5] using both reflection and transmission techniques. The properties of the resonance indicate the existence of a magnetic resonance "bottleneck"—the spin-flip relaxation rate of the conduction electrons to the Mn^{+2} ions exceeds that to the lattice. Previous experiments[2] at what must now be considered rather high Mn concentrations (except those in transmission ESR) were only able to partially open the bottleneck. This was accomplished by increasing the conduction-electron spin-flip lattice relaxation rate upon the addition of nonmagnetic impurities. This provided an effective technique for obtaining the impurity cross section for conduction-electron spin relaxation. As the bottleneck is broken, initially one finds an increase in the ESR thermal broadening coefficient. A complete break would also exhibit a shift in the field for resonance (g shift). No report exists, however, about a change in the Ag:Mn g shift of this origin upon impurity addition.

The purpose of the present work is to report further details of the ESR of dilute Ag:Mn alloys. We have been able to break the bottleneck substantially by using powerful conduction-electron spin-flip "scatterers" (Sb and Au impurities). This provides us with conduction-electron spin-lattice relaxation rates for the scatterers. We also obtain values for the sign and magnitude of the effective local-moment–conduction-electron exchange interaction J from the g-shift and thermal-linewidth measurements. Correlating our results with previous resistivity measurements[6] (especially the coefficient of the Kondo[7] $\ln T$ term) we are able to extract the dependence of J on the momentum-transfer vector $\vec{q}$ for the first three partial waves.[8] The partial-wave analysis can be checked in a critical manner by comparison with the exchange RKKY (Ruderman-Kittel-Kasuya-Yosida) broadening of the host NMR in Ag:Mn dilute alloys. The exchange RKKY interaction as measured by Mizuno[9] and reanalyzed by Alloul[10] is only 25% larger than the value calculated using our three partial-wave amplitudes. These differences are attributed to the large "error bar" in the measured experimental values.

A feature of the ESR experiments on Ag:Mn alloys which has so far eluded quantitative explanation is the ($T=0$) residual linewidth, or the so-called $1/T_{dL}$. It is known from transmission spin resonance (TESR)[5] that this quantity is inversely proportional to the Mn concentration (c), and was interpreted as falling off as $\sim 1/c^2$ at very low c, then as $1/c$ for alloys of greater than 100 ppm Mn (but see discussion in Sec. III C). In our experiments (see also Ref. 3) we have found a nearly equivalent increase in the ESR linewidth extrapolated to zero T as c decreases, or, equivalently, as the bottleneck is progressively broken upon the addition of nonmagnetic impurities. Langreth *et al.*,[11] and then in some detail Pifer and Longo,[12] argued that this might be caused by exchange narrowing of the hyperfine splitting of the Mn^{55}. Quantitative agreement eluded both sets of authors. We are able, at least partially, to account for

the behavior of the residual width $(1/T_{dL})$ by the use of the values for $J(\vec{q})$ as derived from our measurements. We have performed a calculation for the seven (six hyperfine, one conduction electron) exchange-coupled equations of motion, and display the dependence of the full line shape both on c and on temperature. Extraction of an "effective" residual width $1/T_{dL}$ gives values reasonably close to our experimental (ESR) results.

Another feature of the Mn^{55} hyperfine interaction in the dilute noble-metal alloys is the reduction of the hyperfine coupling constant A from the insulator value. Nuclear orientation experiments[13] exhibit a marked reduction in A for Cu as compared to Ag, and for Ag as compared to Au hosts. We attribute this reduction to d-wave admixture. Our measurements in Ag:Mn of $J(\vec{q})$ allow us to estimate the magnitude of the reduction from the insulator value. A comparison with other experiments in Cu:Mn enables us to extract a d-wave scattering approximately twice as large for Cu:Mn as for Ag:Mn. We are able to show that this roughly accounts for the relative change in A between Cu:Mn and Ag:Mn.

The Kondo temperature[7] T_K of the Cu:Mn system has been estimated by Hirschkoff *et al.*[14] to be ~2 mK, while no detectable Kondo condensation has been observed in Ag:Mn by Doran and Symko[15] using a similar method. These numbers are much less than that derived from nuclear orientation studies[13] (25–60 and 40 mK respectively). The interpretation of our results for Ag:Mn, when compared to the interpretation of NMR and transport experiments on Cu:Mn, supports the susceptibility estimates of T_K, as compared to the nuclear orientation estimates.

In Sec. II we present our experimental results. In Sec. III we divide the analysis of these results into three parts: (a) the wave-vector dependence of the exchange in Ag:Mn; (b) the magnitude of the decrease of A upon going from insulating to metallic host; and (c) the line-shape analysis. Section IV compares the results of this paper with previous (some of which are very recent) measurements on Cu:Mn, including the Kondo temperature. Finally, in Sec. V we discuss the differences (and contradictions) between apparently related experiments, and present some suggestions for future research.

II. EXPERIMENTAL RESULTS AND ANALYSIS

The EPR measurements on Ag:Mn were performed at X band, and as a function of temperature in the liquid-helium range $(1.4 \leq T \leq 4.2$ K). The Mn concentration was varied from 50 to 1500 ppm. The samples were prepared by arc-furnace or induction melting, and were examined in powdered form or as single crystals. The experimental results exhibit the following features.

(i) The EPR spectra are a single line, with a linewidth of the form $a+bT$; a and b (residual width and thermal broadening coefficient) depend appreciably on Mn concentration, as well as on other impurities (Sb, Au).

(ii) For small Mn concentrations the g shift is temperature independent. For higher concentrations ($c_{Mn} \geq 250$ ppm), the spectra exhibit ordering effects in that the g shift is slightly positive and temperature dependent.

(iii) Adding Sb impurities increases the g shift and the thermal broadening coefficient. Figure 1 exhibits the effect of Sb addition on g, $b = \Delta H/\Delta T$, and the A/B ratio (in the notation of Feher and

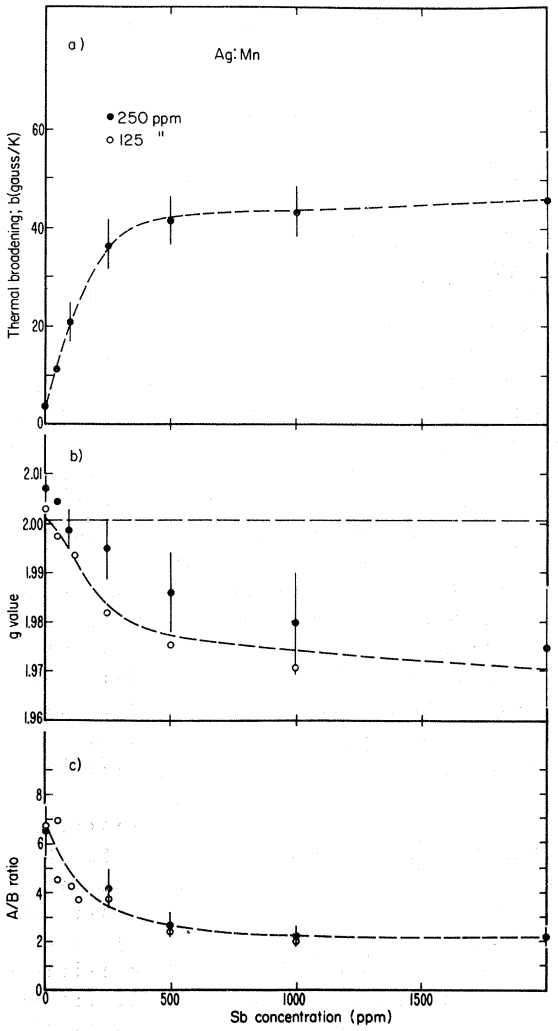

FIG. 1. (a) Thermal broadening, (b) g value, and (c) A/B ratio of the dilute alloy Ag:Mn as a function of antimony (Sb) concentration. The horizontal broken line in (b) represents the Mn g value in insulators. The A/B ratio is defined after Feher and Kip (Ref. 16).

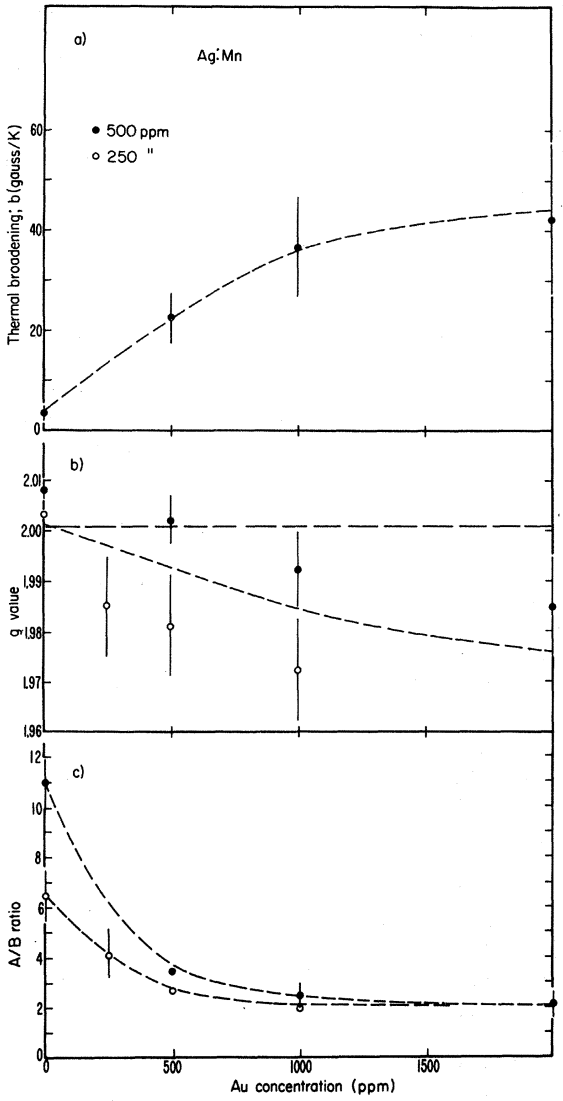

FIG. 2. (a) Thermal broadening, (b) g value, and (c) A/B ratio for the dilute alloy Ag : Mn as a function of Au concentration.

Kip[16]) and Fig. 2 the same for Au addition.

(iv) The A/B ratio and the residual width vary appreciably with Mn concentration. The latter decreases with increasing Mn concentration (Fig. 3) while the former exhibits a peak around 500 ppm [Fig. 4(a)]. The residual width will be discussed in Sec. IIIC. The A/B ratio cannot now be explained.

Features (i) and (iii) of our results are indicative of the presence of a magnetic-resonance bottleneck in the relaxation mechanism.[17] The effect of the Sb or Au is to increase the spin-flip relaxation rate of the conduction electrons via spin-orbit scattering. This process leads to a nearly complete unbottlenecking of the resonance (see Figs. 1 and 2). The bottleneck-broken or "isothermal" limit is characterized in our experimental data by maximum values for both Δg and b which we shall denote Δg_0 and b_0. These maximum values are not changed by further addition of nonmagnetic impurities. According to Figs. 1 and 2, the following values for Δg_0 and b_0 are found:

$$\Delta g_0 = -0.035 \pm 0.01 \,, \qquad b_0 = 45 \pm 10 \text{ G/K} \,. \tag{1}$$

b_0 is related to the exchange spin-flip scattering of the Mn ions, $1/T_{ds}$, given by[17]

$$\frac{1}{T_{ds}} = \frac{\pi}{\hbar}\left\langle\left(\frac{J(q)}{1-U\chi(q)}\right)^2\right\rangle N^2(E_F) K_B T \,; \tag{2}$$

Δg_0 can be expressed as

$$\Delta g_0 = \frac{J(0)}{1-U\chi(0)} N(E_F) \,. \tag{3}$$

Here U is the electron-electron Coulomb interaction responsible for the exchange enhancement of the conduction-electron susceptibility; $J(\vec{q})$ is the $\vec{q}$-dependent exchange interaction; $J(0)$ is the $\vec{q}=0$ component; $\chi(\vec{q})$ is the $\vec{q}$-dependent static susceptibility; $\chi(0)$ is the $\vec{q}=0$ component. The symbol $\langle\ \rangle$ means the normalized sum from $0 \leq |q| \leq 2K_F$ and $N(E_F)$ is the density of states of the conduction electrons per one spin direction at the Fermi energy.

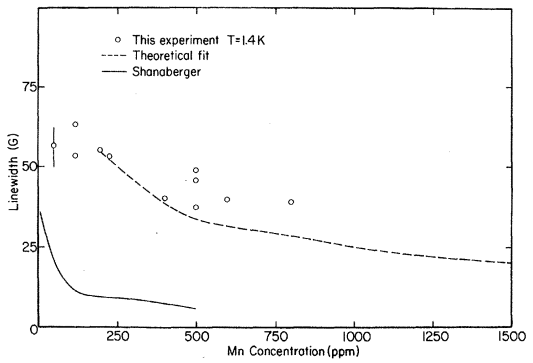

FIG. 3. ESR linewidth of the dilute alloy Ag : Mn as a function of Mn concentration at $T=1.4$ K. The dashed line represents the theoretical fit (at $T=1.4$ K) using the method described in the text, with the same exchange and relaxation parameter as extracted from ESR measurements. We assumed $\delta_{eL} = 3\times10^9 + 9\times10^6\ c_{Mn}$ where c_{Mn} is the Mn concentration in ppm. The hyperfine splitting is 40 G with an enhancement factor of $\alpha = 0.5$. Below 100 ppm a distortion or even a partial resolution (at $T=1$ K) of the line shape was observed in our theoretical line shape and we were not able to extract any linewidth. The solid line represents Shanabarger's (Ref. 5) "residual width" for very dilute Ag : Mn.

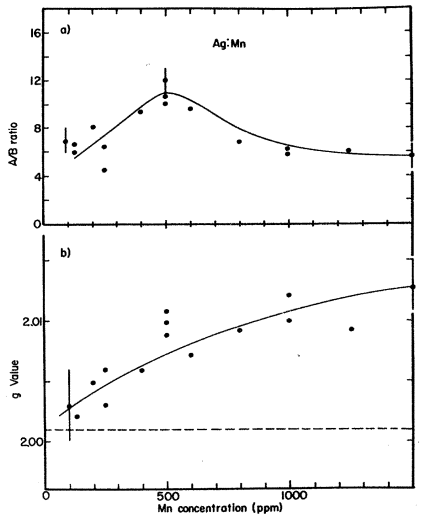

FIG. 4. (a) A/B ratio and (b) the g value as a function of Mn concentration. Both A/B and g were measured at $T = 1.4$ K.

Using $N(E_F) = 0.131$ states/eV atom spin,[18] we find

$$\frac{J(0)}{1 - U\chi(0)} = -0.25 \pm 0.1 \text{ eV}, \tag{4}$$

$$\left\langle \left(\frac{J(q)}{1 - U\chi(q)} \right)^2 \right\rangle = 0.12 \pm 0.03 \text{ eV}^2 . \tag{5}$$

Our "success" in the observation of the isothermal limit as well as the "failure" of previous attempts performed by others[1-5] on Ag:Mn can be explained partially on the basis of choice of the spin-flip scatterer. Usually, the increase of the spin-flip scattering rate upon the addition of impurities is accompanied by an increase in the "residual width." This is probably associated with inhomogeneities in the charge distribution introduced by these impurities. An example of this behavior is provided by a comparison of the effect of Au and Sb impurities on Ag:Mn alloys. Experimentally, the Mn residual width broadens upon the addition of Au much faster than upon the addition of Sb. This also manifests itself by larger error bars in Fig. 2 than in Fig. 1. It should be stressed that the cross section for relaxation by Au impurities (see below) is relatively large, and the bottleneck is expected to be fully broken. However, the accompanying large increase in residual width interferes with the extraction of resonance parameters. Only after breaking the bottleneck using Sb as a scatterer were we able to interpret the Au data. Thus a scatterer is needed which will exhibit the following properties: (a) sufficiently large cross section for conduction-electron–lattice-spin-flip relaxation so that extremely small quantities can open the bottleneck, and (b) only—at worst—a modest increase in the residual width. Information provided by Schultz and Oseroff[18a] indicated that Sb satisfied both criteria. The extraordinary spin-flip efficiency of the Sb scatterer is probably associated either with a p-wave resonance or with the large charge contrast between the Sb (probably Sb^{+5}) and the Ag. The latter results in a substantial attractive potential for the conduction electrons, resulting in a large localized screening charge density. The small ionic radius (0.62 Å) of Sb, as compared to Au, may be the cause of appreciably smaller broadening of the resonance line, but the precise reason is not clear.

It is interesting to compare the spin-flip scattering rates for Sb and Au in Ag. This requires, however, an estimate of the value of the conduction-electron exchange spin-flip scattering rate caused by the Mn ions, $1/T_{sd}$. This scattering rate can be expressed as[16]

$$(1/T_{sd}) = (1/T_{ds})(\chi_d/\chi_s) = (1/T_{ds})(\chi_d/\chi_s^{(0)})[1 - U\chi(0)], \tag{6}$$

where χ_d and $\chi_s^{(0)}$ are the spin susceptibilities of the Mn ions and the unenhanced conduction electrons, respectively. χ_d can be estimated using the Curie-Weiss law with effective spin $S = 2$ (rather than $S = \frac{5}{2}$).[5] $\chi_s^{(0)}$ can be calculated using the free-electron model. There is, however, some disagreement in the literature concerning the value of $U\chi(0)$. The original estimate of Narath[19] yielded $U\chi(0) = 0.47$ for Ag. Later this value was corrected by Narath and Weaver.[20] They found $U\chi(0) = 0.76$ for the δ-function range and $U\chi(0) = 0.33$ for a spatially constant interaction. These calculations are in disagreement with the conduction-electron spin resonance (CESR) of Shanabarger.[5] Shanabarger was able to extract the susceptibility ratio, χ_d/χ_s, from both the g-shift and linewidth behavior in the extreme bottleneck regime, using a Hasegawa-like analysis.[5] He found that χ_s can be very well approximated by a free-electron value without any enhancement. A complication exists, however, in the analysis of Shanabarger. This is caused by the six hyperfine lines arising from the nuclear spin $I = \frac{5}{2}$ of the 100% abundant Mn^{55} isotope. The line-shape analysis to be given in Sec. III C indicates that these lines are not completely narrowed in Shanabarger's experiment. This could slightly change his conclusion. Other evidence for the nonexistence of a large enhancement factor in Ag is provided by correlating reflection and transmission ESR in Ag:Er dilute alloys. A large g shift in the CESR line was observed[21] and attributed[21] to the $\vec{q} = 0$ component of the exchange. This generates an exchange parameter $J(0)$ equal to 0.5 eV for Er in Ag. The Er g shift as measured with respect to the theoretical g value, $g = 6.77$, was found to be $\Delta g = 0.07$.[22]

This g shift can be expressed theoretically by an expression equivalent to (3). We find an enhancement factor very close to zero. Our arguments, however, should be considered with caution. This is because the theoretical value, $g = 6.77$, is actually the Er g value originating with the ground-state orbital momentum of Er^{+3} and corrected for the breakdown of the Russel-Saunders coupling in the free atom. No contribution from covalency was taken into account. Such contributions could change our arguments.

In our analysis we shall therefore consider two extreme cases, $\alpha = U\chi(0) = 0$ and $\alpha = 0.5$.

Using (6) and (5), the conduction-electron exchange spin-flip scattering rate caused by the Mn ions $(1/T_{sd})$ is found to be

$$\frac{\partial(1/T_{sd})}{\partial c} = (3\pm1)\times10^{8}\ \text{sec}^{-1}/\text{ppm Mn} \quad (\alpha=0)$$
$$= (1.5\pm0.5)\times10^{8}\ \text{sec}^{-1}/\text{ppm Mn} \quad (\alpha=0.5)\ . \tag{7}$$

Using these values, the initial slope of the linewidth versus concentration in Figs. 1 and 2 together with the Hasegawa theory[17] yields for the lattice-spin-flip scattering rate

$$\frac{\partial}{\partial c}\left(\frac{1}{T_{sL}}\right)\Big|_{\text{Sb}} = (2.4\pm0.7)\times10^{8}\ \text{sec}^{-1}/\text{ppm Sb} \quad (\alpha=0)$$
$$= (1.2\pm0.4)\times10^{8}\ \text{sec}^{-1}/\text{ppm Sb} \quad (\alpha=0.5). \tag{8}$$

These values are only twice as large as that observed for Au impurities

$$\frac{\partial(1/T_{sL})}{\partial c}\Big|_{\text{Au}} = (1.2\pm0.4)\times10^{8}\ \text{sec}^{-1}/\text{ppm Au} \quad (\alpha=0)$$
$$= (0.6\pm0.2)\times10^{8}\ \text{sec}^{-1}/\text{ppm Au} \quad (\alpha=0.5). \tag{9}$$

Comparing (8) and (9) we see that requirement (a) was in fact satisfied in previous experiments using Au as an impurity. Failure to satisfy (b) was the only reason why clear evidence of a g shift was absent from previous experiments in which the bottleneck was partially broken.

III. ANALYSIS

A. Wave-vector dependence of the exchange

According to Davidov *et al.*,[8] we can write (see also Blandin[23])

$$J(\vec{q}) = \sum_{L=0}^{\infty}(2L+1)J^{(L)}P_L(\cos\theta)\ , \tag{10}$$

where $|q| = k_F[2(1-\cos\theta)]^{1/2}$ and $\cos\theta = (\vec{k}\cdot\vec{k}'/|\vec{k}|\,|\vec{k}'|)$. The expression (10) is correct only if the Fermi surface is spherical, and only for $|\vec{k}|$, $|\vec{k}'| = k_F$, i.e., for scattering on the Fermi surface. Our principal aim is to use the g-shift [Eq. (4)] and linewidth [Eq. (5)] results to obtain the partial-wave amplitudes $J^{(L)}$. In the presence of exchange enhancement (4) and (5) can be expressed, using a partial-wave analysis, as[24]

$$J_{\text{eff}}(0) = \frac{J(0)}{1-U\chi(0)} = (J^{(0)} + 3J^{(1)} + 5J^{(2)} + \cdots)\frac{1}{1-U\chi(0)}, \tag{11}$$

$$\langle[J_{\text{eff}}(\vec{q})]^2\rangle = \left\langle\left(\frac{J(\vec{q})}{1-U\chi(\vec{q})}\right)^2\right\rangle$$
$$= \Sigma_{LL'}(2L+1)(2L'+1)(J^{(L)})(J^{(L')}) \times\left\langle\frac{P_L(\cos\theta)P_{L'}(\cos\theta)}{[1-U\chi(\cos\theta)]^2}\right\rangle\ . \tag{12}$$

In the absence of enhancement the cross terms $(L \neq L')$ in (12) vanish, and results identical to those in Ref. 8 are obtained. Equations (11) and (12) give two relations between $J^{(L)}$. From our previous work[8] we expect only $L = 0$, 1, and 2 terms to be significant for transition-metal impurities (see below). We therefore need at least one further relation to obtain a set of explicit values for the $J^{(L)}$. We turn to transport measurements, where we have previously shown that,[8] in the absence of potential scattering (Fischer gives the complete expression[7]), the electrical resistivity can be written as

$$\rho = \frac{2\pi N(E_F)mcS(S+1)}{zN_0e^2\hbar}\left[\langle[J_{\text{eff}}(\vec{q})]^2(1-\cos\theta)\rangle + 4N(E_F)\ln\left(\frac{k_BT}{D}\right)\langle[J_{\text{eff}}(\vec{q})]^3(1-\cos\theta)\rangle\right]$$
$$= \frac{2\pi N(E_F)mcS(S+1)}{zN_0e^2\hbar}\left[[(J^{(0)}-J^{(1)})^2 + 2(J^{(1)}-J^{(2)})^2 + 3(J^{(2)})^2] + 4N(E_F)\ln\left(\frac{k_BT}{D}\right)[(J^{(0)}+J^{(1)})(J^{(0)}-J^{(1)})^2 + 2(J^{(1)}+J^{(2)})(J^{(1)}-J^{(2)})^2 + 3(J^{(2)})^3]\right]\ . \tag{13}$$

Here $N(E_F)$ is the one-spin conduction-electron density of states at the Fermi energy, S the spin of the paramagnetic impurity, z the number of conduction electrons per atomic cell, D the bandwidth, and N_0 the number of atomic cells per unit volume.

The three expressions (11), (12), and (13) in principle overdetermine the s-, p-, and d-partial-wave contributions to $J(\vec{q})$. However, the available electrical resistivity data on Ag:Mn are not reliable for the normal, or J^2, term in (13). Magnetoresistance measurements, which could yield reliable values for this term by virtue of their ability to separate potential from spin-flip

scattering contributions to ρ, have only been carried out for Cu:Mn by Monod.[25] This limits us to use only of the $\ln T$ term, but we are able to determine the s-, p-, and d-wave contributions. Using the value of Jha and Jericho[6] for the coefficient of the $\ln T$ term, and neglecting potential scattering,[7] we find

$$\langle [J_{\rm eff}(\vec{q})]^3(1-\cos\theta)\rangle = 0.0096 \text{ eV}^3 . \quad (14)$$

Our analysis proceeds as follows. We note that $J^{(L)} = J^{(L)}_{\rm At} + J^{(L)}_{\rm CM}$, where $J^{(L)}_{\rm At} > 0$ for all L under our conditions, and $J^{(L)}_{\rm CM} < 0$. The subscripts At and Cm represent the atomic Coulomb and covalent mixing contributions, respectively. According to Watson,[8]

$$J^{(0)}_{\rm At} > J^{(1)}_{\rm At} > J^{(2)}_{\rm At} , \quad (15)$$

though the last may be somewhat enhanced[8] by virtue of the Clebsch-Gordan coefficients. Also, for $3d$ transition-metal ions,

$$|J^{(2)}_{\rm CM}| \gg |J^{(0)}_{\rm CM}| , \quad (16)$$

with $J^{(1)}_{\rm CM}$ and $J^{(3)}_{\rm CM}$ completely negligible. These conditions are a consequence of the nearly spherical character of the Hartree-Fock mixing potential. $J^{(0)}_{\rm CM}$ depends on its quadrupolar character, which is expected to be small, and $J^{(L)}_{\rm CM}$, L odd, depends on the odd-parity components of the mixing potential, and these are known to be negligible.

We therefore expect $J^{(0)}$ to be positive, though perhaps reduced because of the partial cancellation of $J^{(0)}_{\rm At}$ (positive) by the (negative) $J^{(0)}_{\rm CM}$. $J^{(1)}$ must be positive (this will be important below) and $J^{(2)}$ can be of either sign. For transition-metal ions it is now generally accepted that the intrinsically small value of $J^{(2)}_{\rm At}$, coupled with the full force of the interband mixing, expressed through $J^{(2)}_{\rm CM}$, is sufficient to result in a negative value of $J^{(2)}$. Indeed, if such were not the case, the Kondo anomaly would not be present.

As demonstrated above, the exact enhancement factor in Ag is not known, although it is believed to be small. In addition, the "error bars" in the exchange interactions (4) and (5) are approximately 30%. Large error bars exist also in the exchange parameter (14) extracted from resistivity. This is because the coefficient in the $\ln T$ term in the electrical resistivity appears to vary with concentration. It increases upon decreasing solute concentration by 20% from 70 to 50 ppm. In the presence of such large error bars in the measured values we shall neglect enhancement altogether. When we carry out our fitting procedure, using (4), (5), and (14) in (11), (12), and (13), respectively, the most satisfactory set of partial-wave amplitudes is found to be

	$J^{(0)}$ (eV)	$J^{(1)}$ (eV)	$J^{(2)}$ (eV)
Ag:Mn	+0.13	+0.09	−0.13 . (17)

We can check the consistency of these partial waves using the host NMR line broadening caused by RKKY conduction-electron polarization induced by the magnetic impurity. The host NMR broadening of Ag in Ag:Mn dilute alloys was measured by Mizuno.[9] However, he used an incorrect value of the hyperfine constant for Ag, and therefore extracted too large a value for $J_{\rm eff}$(RKKY). Alloul,[10] using the value derived by Bennett *et al.*,[26] extracted $|J_{\rm eff}(\text{RKKY})N(E_F)| = 0.147 \pm 0.013$, where $N(E_F)$ is the one-spin conduction-electron density of states at the Fermi level. Using $N(E_F) = 0.131$ states/eV, we would find

$$|J_{\rm eff}(\text{RKKY})| = 1.12 \pm 0.10 \text{ eV} . \quad (18)$$

The problem with this value is that the raw data from which it was extracted exhibit a curious curvature for large values of $\langle S^z \rangle$ which Mizuno was unable to explain (this was pointed out to us by Walstedt). Thus, some uncertainty enters into (18), and one should regard it as only an upper limit.

As shown in Refs. 8 and 24 (see also Appendix B), the effective exchange has the form

$$J_{\rm eff}(\text{RKKY}) = \frac{\Sigma_L (2L+1)(-1)^L J^{(L)}}{[1-(1/2)U\chi(0)]^2} , \quad (19)$$

where the enhancement factor in (19) was first discussed in principle by Blandin,[23] and then in detail independently by Walker and Walstedt.[24]

Using (17), we evaluate (19) [again assuming $U\chi(0) = 0$] to find

$$J_{\rm eff}(\text{RKKY}) = -0.79 \text{ eV} . \quad (20)$$

This value is about 25% smaller than the experimental result (18). In view of the uncertainties in the various measured values, as well as the approximate nature of the theory, we are not overly concerned by this difference. The main point is how one can correlate the exchange parameters as extracted by different experimental techniques using a partial-wave analysis. We were partially successful [assuming $U\chi(0) = 0$] as demonstrated above. For the case of $U\chi(0) = 0.5$ the agreement is much worse. The $\vec{q}$ dependence of the exchange using (10) and (17) is exhibited in Fig. 5.

The results (17) have an immediate consequence for the hyperfine field and Kondo temperature for Ag:Mn, and will be discussed further in Secs. III B and IV, respectively.

B. Hyperfine field

The Mn^{55} hyperfine field in the dilute alloy Ag:Mn is nearly half that found in insulators[13]

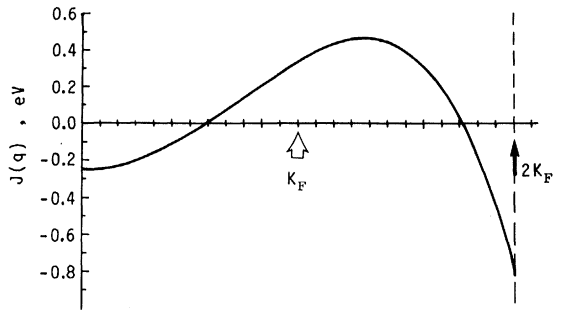

FIG. 5. q dependence ($q=\vec{k}-\vec{k}'$) of the exchange interaction [$J(q)$] for Mn in Ag as calculated from (10) using (17).

(− 330 and − 460 kG, respectively). In the latter, its origin is now known to result from polarization of the occupied s-electron cores by the unpaired d-electron spin. The sign is negative, arising from the attractive exchange potential between the inner s shells and the d spins. The large reduction in metals is believed to be caused by a positive dynamic conduction-electron polarization in the vicinity of the localized moment. Yosida[27] was the first to calculate this polarization and its contribution to the hyperfine field at the nucleus of the magnetic impurity. Extending (very slightly) the work of Hirst,[28] the change in the EPR hyperfine coupling constant can be shown to equal

$$\Delta A=\sum_{\vec{k},\vec{k}'}\frac{J(\vec{k},\vec{k}')A(\vec{k}',\vec{k})+\text{c.c.}}{\epsilon_{\vec{k}'}-\epsilon_{\vec{k}}}f_{\vec{k}}(1-f_{\vec{k}'})\,, \qquad (21)$$

where we have allowed for a hyperfine field form factor, as is surely the case for core polarization. The conduction electron's contribution to the hyperfine field at the nucleus is obtained from (21) by multiplication by the factor $\langle S^z\rangle/g_e\mu_e$. Only if *both* $J(\vec{k},\vec{k}')$ and $A(\vec{k},\vec{k}')$ are independent of $\vec{k}$ and $\vec{k}'$ can (21) be reduced to the familiar form[29]

$$\Delta A=\tfrac{1}{2}(A^{(0)}J^{(0)}+3A^{(1)}J^{(1)}+5A^{(2)}J^{(2)})N(E_F)\,, \qquad (22)$$

where $A^{(L)}$ is the hyperfine coupling constant appropriate to the Lth partial wave. Conduction electrons with s-wave character contribute to the hyperfine interaction via the (positive) contact term; while those of p- or d-wave character contribute via the (negative) core polarization mechanism. From (17) we see that the s- and p-wave exchange is positive, while the d wave is negative for Ag:Mn. Allowing for the degeneracy factors, one can safely ignore the p-wave contribution to A. The combination of positive hyperfine interaction and exchange for s waves, and negative hyperfine interaction and exchange for d waves, leads therefore to a positive increase in the polarization-induced hyperfine interaction from both sources. If for some reason our analysis were in error, and $J^{(0)}$ were predominant and negative, the change in hyperfine interaction from s waves would have been negative. This would lead to a negative conduction-electron contribution to the hyperfine field because the magnitude of $A^{(0)}$ is much larger than that of any $A^{(L)}$ ($L\geq 1$). This would be in disagreement with the experimental hyperfine fields quoted above.

To get a feeling for the relative contributions to ΔA in (22), we use the measured difference (+130 kOe) between the insulator and alloy (Ag:Mn) value for $H_{\text{hyp}}=AS/g_N\mu_N$. Using $H_{\text{hyp}}^{(s)}=6\times10^6$ kOe for $4s$-like electrons,[30] we find that the s wave's contribution is approximately 40% of the measured ΔA for Ag:Mn. We would then extract a value for the d-spin-polarization hyperfine contribution, which, after allowing for degeneracy, would have to correspond to one-third of the s-spin-polarization hyperfine field. This is much too large, and one must use such values with great caution. This is a consequence of $\vec{k}$ and $\vec{k}'$ in (21) *not* being restricted to the Fermi surface. The partial-wave analysis is no longer reliable; $J^{(L)}$ is no longer constant but varies with $\epsilon_{\vec{k}}$ and $\epsilon_{\vec{k}'}$, not to mention the variation of $A(\vec{k},\vec{k}')$. Applying values obtained for the exchange parameter from magnetic resonance or transport measurements (where $\vec{k}$ and $\vec{k}'$ are restricted to the Fermi surface) and using these values to obtain changes in the hyperfine constant (where k and k' vary over all k space, subject only to the exclusion-principle restrictions) should not be taken too seriously.

C. Line-shape analysis

In this section we analyze the expected ESR line shape for Ag:Mn in the presence of exchange (Sec. III A) and hyperfine interaction (Sec. III B). Two anomalous features are observed for dilute Ag:Mn alloys. First, the residual width decreases with increasing Mn concentration (Fig. 3). This is in marked contrast to observations in most other dilute alloys. Second, the Mn A/B lineshape ratio decreases upon addition of other nonmagnetic impurities (Fig. 1, Sb; Fig. 2, Au) but exhibits a clear maximum as a function of Mn concentration [Fig. 4(a)]. The first feature has been observed in transmission electron spin resonance in both Ag:Mn and Cu:Mn.[5] No satisfactory explanation has been given, however.

In an attempt to interpret these features we have performed a line-shape analysis similar to that of Pifer and Longo.[12] This analysis is necessary because the six hyperfine lines ($I=\frac{5}{2}$ for Mn^{55}) are presumably almost completely exchanged narrowed in our experiment.

We start with seven Hasegawa-type equations

of motion: six for the magnetizations, $\vec{M}_\kappa$, associated with the six hyperfine lines ($\kappa = 1, 2, \ldots, 2I+1$), and the seventh associated with the conduction electron's magnetization, $\vec{M}_s$. These equations can be written as

$$\frac{d\vec{M}_\kappa}{dt} = \gamma[\vec{M}_\kappa \times (\vec{H} + \vec{H}_\kappa^{\rm hf} + \lambda \vec{M}_s)] + \frac{1}{6T_{sd}} \times \left[\vec{M}_s - \chi_s^{(0)}\left(\vec{H} + \lambda \sum_{\kappa'=1}^{6} \vec{M}_{\kappa'}\right)\right] - \left(\frac{1}{T_{ds}} + \frac{1}{T_{dL}}\right)\left(\vec{M}_\kappa - \frac{\chi_d}{6}(\vec{H} + \lambda \vec{M}_s)\right), \quad (23)$$

$$\frac{d\vec{M}_s}{dt} = \gamma\left[\vec{M}_s \times \left(\vec{H} + \lambda \sum_{\kappa=1}^{6} \vec{M}_\kappa\right)\right] + \frac{1}{T_{ds}} \times \left(\sum_{\kappa=1}^{6} \vec{M}_\kappa - \chi_d(\vec{H} + \lambda \vec{M}_s)\right) - \left(\frac{1}{T_{sd}} + \frac{1}{T_{sL}}\right) \times \left[\vec{M}_s - \chi_s\left(\vec{H} + \lambda \sum_{\kappa=1}^{6} \vec{M}_\kappa\right)\right] \quad (\kappa = 1, 2, \ldots, 6), \quad (24)$$

where $1/T_{ds}$ and $1/T_{sd}$ are the exchange spin-flip relaxation rates of the paramagnetic impurities to the conduction electrons, and vice versa, respectively; χ_s and χ_d are the spin susceptibilities of the conduction electrons and the paramagnetic impurities, respectively; H is the external magnetic field, γ the gyromagnetic ratio (assumed to be the same for both spin species); $1/T_{dL}$ and $1/T_{sL}$ the spin-flip relaxation rates of the paramagnetic impurities and conduction electrons to the lattice, respectively; $H_\kappa^{\rm hf}$ is the hyperfine field acting on the magnetization associated with the κth hyperfine line; and λ is the exchange coupling constant related to $J(0)$ (see below for the explicit form). The equations of motion (23) and (24) are similar to those suggested previously by Cottet *et al.*,[31] where relaxation is toward the instantaneous local field.

The line shape was generated by calculating the transverse susceptibilities $\chi_\kappa^+(H)$, $\kappa = 1, 2, \ldots, 6$, and $\chi_s^+(H)$. The total transverse susceptibility $\chi^+(H)$, defined as

$$\chi^+(H) = \left(\sum_{\kappa=1}^{6} \chi_\kappa^+(H)\right) + \chi_s^+(H), \quad (25)$$

was determined by a solution of the matrix equation (see Appendix A). The actual line shape is given by plotting $\mathrm{Re}\chi^+(H)$ as a function of H. The line shape depends explicitly on the parameters χ_d, χ_s, λ, $1/T_{ds}$, $1/T_{dL}$, $1/T_{sL}$, and $H_\kappa^{\rm hf}$.

The unenhanced electron spin susceptibility, $\chi_s^{(0)}$, was estimated to be $\chi_s^{(0)} = 0.7 \times 10^{-5}$ emu/mole. We used a Ag density of states $N(E_F) \cong 0.131$-states/eV atom spin. In the presence of electron-electron Coulomb interaction responsible for the enhancement, the conduction-electron spin susceptibility χ_s can be expressed as

$$\chi_s = \frac{\chi_s^{(0)}}{1 - U\chi_s^{(0)}}. \quad (26)$$

A Curie law was taken for χ_d (with $S = 2$) in which both Mn concentration and temperature are explicit parameters depending on the experimental conditions. The parameter λ is related to the exchange interaction and can be written as[17]

$$\lambda = \frac{J(0)}{g^2 \mu_B^2 N_0}. \quad (27)$$

The parameter $1/T_{dL}$ is assumed to be equal to the "residual width" for each hyperfine line. To estimate $1/T_{dL}$ we assumed that the ESR spectra were almost completely exchange narrowed, such that the standard Hasegawa expression[17] (in the absence of hyperfine interaction) was a reasonable approximation. The value of $1/T_{sL}$ was taken from our results or, where appropriate, from Shanabarger.[5] Finally, the hyperfine field $H_\kappa^{\rm hf}$ for different κ values was extracted from a hyperfine constant of 40 G. A similar value was observed for Ag : Mn alloys by Okuda and Date.[4] The hyperfine constant for Cu : Mn would be slightly smaller (~30 G), as exhibited in nuclear orientation measurements.[13]

Figure 6 exhibits the theoretical line shape for (a) zero exchange interaction, (b) negative exchange interaction but in the bottleneck regime, and (c) the same exchange but without a bottleneck (i.e., $1/T_{sL} \gg 1/T_{sd}$). The various parameters used for these plots are quoted in the caption of Fig. 6. It is clearly seen that "turning on" the exchange interaction completely narrows the six hyperfine lines into a single line for the Mn concentration range appropriate to our experiments. The Mn concentration used for these plots is sufficiently large that the oscillator strength associated with the conduction-electron spin-resonance line can be neglected. The effect of increasing $1/T_{sL}$ is to shift and broaden the line [Fig. 6(c)].

Several physical mechanisms for exchange narrowing, two of which are contained implicitly in (23), may be of importance.

(a) The "bottleneck mechanism" previously proposed by Barnes *et al.*[32] This mechanism makes use of the fact that in the bottleneck regime the transverse magnetization associated with the Mn hyperfine lines and the conduction electrons are locked together in phase. Thus, a coherent magnetization transfer (at a rate of $1/T_{ds}$) takes place between the various hyperfine lines, leading to a narrowing. This mechanism is almost independent of Mn concentration in the extreme bottleneck regime.

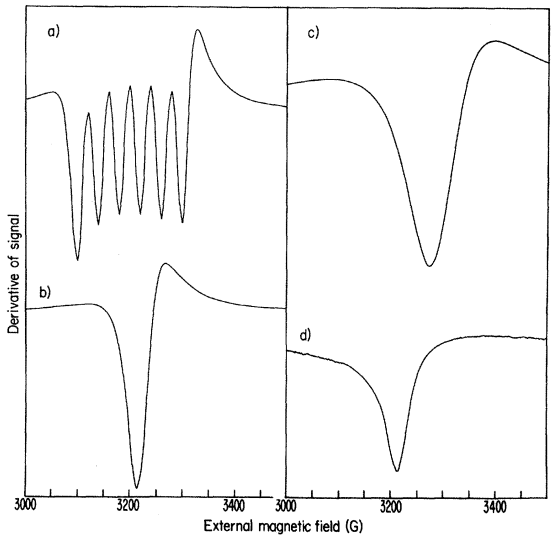

FIG. 6. Theoretical line shape calculated for $c_{Mn}=500$ ppm in the cases (a) zero exchange parameter $J_{eff}=0$, $\langle J^2_{eff}(q)\rangle=0$, (b) the exchange as extracted from our ESR measurements but using a value of $1/T_{sL}$ much smaller than $1/T_{sd}$ (bottleneck regime, $1/T_{sL}=0.34\times10^{11}$ sec^{-1}, $1/T_{sd}=0.15\times10^{12}$ sec^{-1}), (c) using a value of $1/T_{sL}$ appropriate to the unbottleneck regime ($1/T_{sL}\gg1/T_{sd}$, $1/T_{sL}=0.1\times10^{13}$ sec^{-1}, $1/T_{sd}=0.15\times10^{12}$ sec^{-1}), (d) representing the experimental observed line shape for $c_{Mn}=500$ ppm at $T=1.4$ K. The individual hyperfine line shape was assumed to be Dysonian with A/B ratio equal to 6.

(b) The second term in the equations of motion, (23), shows that the transverse magnetization, M^+_κ, can be transferred to any other magnetization $M^+_{\kappa'}$, at a rate $\lambda\chi_e(1/6T_{sd})$ (see also Appendix A). This occurs even in the absence of bottleneck effect and provides an important narrowing mechanism that cannot be neglected. It originates with the requirement that the relaxation is toward the instantaneous local field. Such a requirement creates some coherence (or memory) between transverse magnetizations associated with different hyperfine lines. This mechanism is temperature independent but concentration dependent (opposite to that of the bottleneck mechanism) and depends on the sign of the exchange.

(c) The effect of a Ruderman-Kittel spin-spin exchange interaction between the Mn ions on the hyperfine splitting has been treated by Barnes.[33] This narrowing mechanism behaves similarly to that described in (b) in the sense that it is temperature independent but proportional to the Mn concentration. Resistivity[6] measurements, as well as our g-shift results [Fig. 4(b)], indicate interaction effects only for concentrations in excess of 250 ppm. At lower concentrations, interactions cannot be responsible for the narrowing of the hyperfine spectrum, and we can therefore look for "single impurity" effects. The physics contained in (23) and (24) is just of this type.

The calculated line shapes were analyzed by the method of Peter *et al.*[34] This was possible, however, only close to the extreme narrowing regime where the line shape could be approximated roughly by a Lorentzian line shape. The experimental line shapes which led to Figs. 1–4 were analyzed in the same manner. The analysis yielded the following features.

(i) It was found that the linewidth does not always increase linearly with increasing temperature, but frequently exhibits different slopes at high ($T\geq5$ K) and low temperatures (the calculations were carried out in the temperature range $0.5\leq T\leq30$ K). Thus, a complication exists in the extraction of the "residual width" from the calculated line shape. Our experiments, however, were performed only in the temperature range $1.4\leq T\leq4.2$ K and linearity of the theoretical linewidth versus temperature was always found in this limited range.

(ii) Because of the complication mentioned in (i), rather than comparing the experimental "residual width" with the theoretical one, we prefer to compare the full linewidths themselves at a given temperature. This was carried out in Fig. 3, where the experimental linewidth of Ag:Mn at $T=1.4$ K is plotted as a function of Mn concentration. For comparison, the "residual width" of Ag:Mn dilute alloys as extracted by Shanabarger[5] is also exhibited in the same figure. The theoretical line shape is represented by the dashed line. The exchange parameters used are those found in Sec. III A. The value of "$1/T_{dL}$" is assumed to be 3×10^8 sec^{-1} (corresponding to an individual residual width of ~15 G), with the value of $1/T_{sL}$ as extracted by Shanabarger for low Mn concentration and modified by us to our experimental conditions. We were not able to extract any meaningful linewidth from the theoretical spectra for low Mn concentrations (less than 100 ppm). This is because of partial resolution of the spectra or very large deviation from a Lorentzian line shape.

(iii) The partial resolution observed for low concentration (lower than 50 ppm and at a temperature of 0.5 K) (see Fig. 7) confirms the prediction of Barnes *et al.*[32] These authors predict the possibility of partial resolved hyperfine structure even in the presence of bottleneck effect. It should be stressed, however, that signal-to-noise and temperature considerations make the experiment difficult, and so far we have not been successful in observing these effects.

Unfortunately, the theory is incapable of explaining the behavior of the A/B ratio in Fig. 4. It should be mentioned that in our line-shape analysis, no second-order hyperfine corrections were

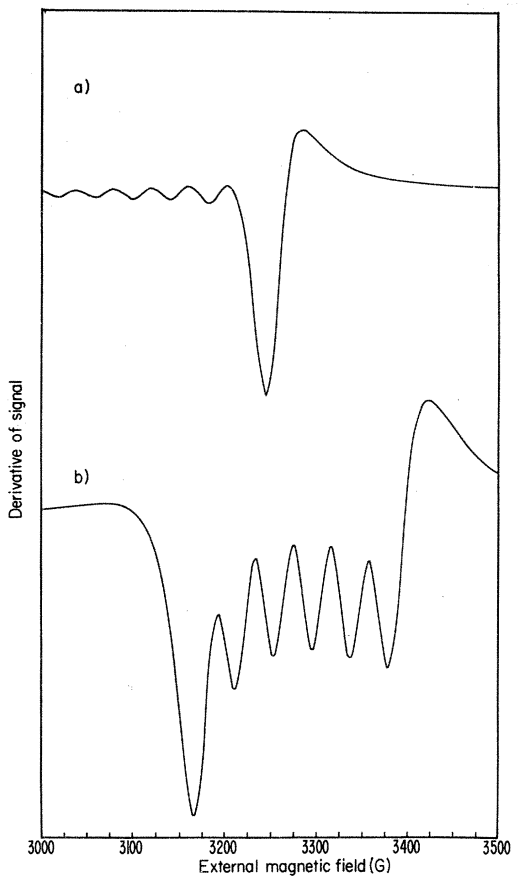

FIG. 7. Theoretical line shape calculated at $T=0.5$ K for the cases (a) $c_{\mathrm{Mn}}=50$ ppm and $1/T_{sL} \gg 1/T_{sd}=0.3\times10^{11}$ sec^{-1} (weak-bottleneck regime), (b) $c_{\mathrm{Mn}}=10$ ppm and $1/T_{sL}=0.3\times10^{11}$ sec^{-1}, $1/T_{sd}=0.3\times10^{10}$ sec^{-1} (unbottleneck regime).

introduced. Such corrections could conceivably change the center of gravity of the hyperfine lines, and might therefore affect the A/B ratio because of nonsymmetric field distribution, but we would expect the net effect to be small.

IV. COMPARISON WITH Cu : Mn

Preliminary ESR measurements in the analog system Cu:Mn "failed" to exhibit an "unbottlenecked" g shift and thermal broadening. A possible reason for this will be discussed below. In the absence of such information (from ESR) it is instructive to compare our results for Ag:Mn with those found by others for Cu:Mn. We have already noted that nuclear orientation experiments[13] show a smaller hyperfine field for Cu:Mn as compared to Ag:Mn, indicating an increase in either $J^{(0)}$ or $J^{(2)}$ of the former as compared to the latter. One expects that J_{At} should remain roughly constant as one changes host. This implies that it is the increase of $|J_{\mathrm{CM}}|$ which is responsible for the diminution of A. Hence we expect $J^{(2)}$ to be larger (negatively) for Cu:Mn than for Ag:Mn, with $J^{(0)}$ if anything smaller. In addition, the Kondo "temperature" has been determined[14] for Cu:Mn as approximately 2 mK. For[15] Ag:Mn it appears to be substantially below 1 mK. The rapid dependence of T_K on $J^{(2)}$ implies that this difference might also be understood on the basis of our partial-wave analysis.

In attempting to extract the $J^{(2)}$ from Cu:Mn we are limited to measurements of the impurity NMR,[35] which gives $1/T_{ds}$, to host NMR,[23] which gives the coefficient of the long-range part of the RKKY interaction (and also a measure of $1/T_{ds}$), and to magnetoresistance measurements,[25] which yield the coefficient of the J^2 contribution to ρ [see Eq. (13)]. These data can be summarized as follows:

$$\text{Impurity NMR (Ref. 35)} \qquad \langle J^2_{\mathrm{eff}}(q)\rangle^{1/2}=1.2 \text{ eV}; \tag{28}$$

$$\text{Host NMR (Ref. 23)} \qquad |J_{\mathrm{eff}}(\mathrm{RKKY})|=1.65 \text{ eV} \tag{29}$$

$$\text{Magnetoresistance (Ref. 25)} \qquad \langle J^2_{\mathrm{eff}}(1-\cos\theta)\rangle^{1/2}=0.8 \text{ eV}. \tag{30}$$

The right-hand side of (30) has been corrected by Beal-Monod and Wiener[36] to be 0.66 or 0.48, depending on whether one omits or includes the J^3 terms in the full analysis of the magnetoresistance. We shall use these values below.

The enhancement factor for Cu has been found by Walstedt and Yafet[37] to be $\alpha=0.1$. This agrees also with the CESR results of Shanabarger[5] as well as those of Hundquist and Monod[38] using implanted samples of Cu:Mn. Assuming also $J^{(0)}$ and $J^{(1)}$ to be the same as in Ag, one would find

$$\text{Impurity NMR} \qquad J^{(2)} \cong -0.48 \text{ eV}; \tag{31a}$$

$$\text{Host NMR} \qquad J^{(2)} \cong -0.28 \text{ eV}; \tag{31b}$$

$$\text{Transport} \qquad |J^{(2)}| \cong 0.3 \text{ eV} \cong 0.22 \text{ eV}. \tag{31c}$$

It is seen that the host NMR falls within the range of the transport measurement value, but the impurity NMR value is nearly twice as large as that extracted from the other two methods.

It should be stressed also that preliminary line-shape analysis using a value of $\langle J^2\rangle^{1/2}=1.2$ eV and hyperfine constant of 30 G, as well as Shanabarger's parameters for Cu:Mn, indicates that the spectra are completely exchange narrowed. The experimental results of Shanabarger exhibit, however, a decrease of the residual with increasing Mn concentration, even for Cu:Mn dilute alloys. Thus, the impurity NMR value of 1.2 eV for $\langle J^2\rangle^{1/2}$ seems to be too large. Finally, magnetization measurements[14,15] indicate that the paramagnetic Curie temperature (due to spin-spin

interaction) is only 2.5 times larger in Cu:Mn than it is in Ag:Mn for the same Mn concentration. Since the paramagnetic Curie temperature is proportional to the square of the effective Mn conduction-electron exchange interaction, and the impurity NMR $J^{(2)}$ is 3.7 times our value for $J^{(2)}$ in Ag:Mn, we have further evidence that the impurity NMR value may be too great.

It is of interest to use the value for $J^{(2)}$ in (17) to estimate T_K for Ag:Mn. We take[7] $T_K = D\{\exp 1/[J^{(2)}N(E_F)]\}$, where D is the bandwidth. If one takes D to be the same for Cu and Ag doped with Mn, then using the smallest limit on $|J^{(2)}|$ from (31), and taking $J^{(2)} = -0.13$ eV for Ag:Mn from (17), one finds

$$T_K(\mathrm{Ag:Mn}) \cong T_K(\mathrm{Cu:Mn}) \times 10^{-13} \sim 2 \times 10^{-16}\ \mathrm{K}\,. \tag{32}$$

The ratio (32) was calculated assuming (31b) and (17). It should be stressed, however, that the error bar in (31b) and (17) is relatively large. A change in $J^{(2)}$ of 40% can change our value of T_K by several orders of magnitude. Equation (32) should be therefore considered with caution. It is certainly clear, however, why Doran and Symko[15] failed to observe the effect of the Kondo condensation in Ag:Mn magnetic susceptibility measurements.

It is also worthwhile to point out that the reduction in hyperfine coupling from Ag:Mn to Cu:Mn is very roughly given by the smaller of the exchange values in (27). While the insulator value is ~ -460 kOe, the value for Cu:Mn is -280 kOe and for Ag:Mn -330 kOe. We have already shown that s-wave contributions cause ~40% of the reduction in H_{hyp} between the insulator value and that found in Ag:Mn. If we keep the absolute magnitude of the s-wave contribution the same in Cu:Mn as we used for Ag:Mn, and (with great doubt) make use of (22) keeping $A^{(2)}$ fixed, we would calculate from the change in hyperfine field $J^{(2)} = -0.2$ eV. This value actually agrees with the magnetoresistance value of Monod[25] as analyzed by Beal-Monod and Weiner[36] with the J^3 terms included.

V. DISCUSSION

In summation, we have broken the bottleneck in Ag:Mn and used the g shift and thermal linewidth to obtain the spin-orbit spin-flip scattering rates for Sb and Au impurities, and the related values of the exchange coupling. The transport measurements of Jha and Jericho,[6] taken together with the latter, lead to a set of partial-wave amplitudes, positive for s and p waves, and negative for d waves. The impact of these amplitudes on the change in hyperfine field upon going from the insulator to the metal, and the shape of the ESR line in the presence of hyperfine splitting, were examined. Comparison was made with the results of related experiments in Cu:Mn, and it was argued that, at most, $J^{(2)}$ could exceed the value in Ag:Mn by a factor of 2–3. This was sufficient, however (working backwards), to show that T_K was negligibly small for Ag:Mn.

The prospects appear dim for breaking the bottleneck in Cu:Mn as $1/T_{ds}$ is four to five times that of Ag:Mn (putting it in the vicinity of 200 G/K). Thus, only at He^3 temperatures could one hope to observe the bottleneck-broken line. However, things are actually even worse (see Ref. 39). Because $1/T_{ds}$ is larger, so also is the bottleneck controlling $1/T_{sd}$. Thus, the concentration of the second impurity ("spin-flip scatterer") needed to break the bottleneck is much larger in Cu:Mn as compared to Ag:Mn. At such a large impurity concentration, appreciable inhomogeneous broadening of the Mn signal would occur. This would add to the thermal exchange broadening, and make the extraction of meaningful parameters almost impossible.

Finally, there is an interesting complementarity between the ESR of Mn in Cu:Mn and Ag:Mn, and the NMR of Mn^{55} by Walstedt and Warren.[35] These authors were able to observe the NMR of Cu:Mn^{55} in the paramagnetic state at high temperatures. They "failed," however, to detect the resonance in Ag:Mn dilute alloys. The reason is probably associated with the magnitude of $\langle J^2_{\mathrm{eff}}(\vec{q})\rangle$.[40] NMR detection is favorable in dilute alloys exhibiting large exchange. The opposite is true for the ESR experiments, where the unbottlenecked linewidth is directly proportional to $\langle J^2_{\mathrm{eff}}(\vec{q})\rangle$. Breaking the bottleneck is more favorable for alloys having small values of this parameter. Thus ESR and high-temperature NMR are complementary techniques.

ACKNOWLEDGMENTS

The authors wish to acknowledge Professor S. Shultz and Dr. S. Oseroff for very important information and discussions concerning Ag:Mn and Cu:Mn dilute alloys, and the very great assistance of Professor K. Maki in the early stages of this work. We are especially indebted to Dr. R. E. Walstedt for many discussions during the progress of this research, for generously providing us with his computer results for Eq. (12) prior to publication, and for pointing out the difficulties associated with the interpretation of the host NMR data as remarked in the text. We thank D. Rittenberg for the preliminary line-shape analysis and Dr. H. Alloul, Dr. P. Monod, and Dr. H. Hundquist for helpful discussions with regard to the re-

lationship between the different experimental determinations of the exchange. Dr. P. Chaikin and Dr. M. R. Shanabarger are gratefully acknowledged for discussions in various stages of this work. We thank S. Gillespie for the line-shape computer work. We are indebted to Dr. Alloul and Dr. Walstedt for pointing out to us the error rectified in Appendix B.

APPENDIX A

The transverse part of $\chi^+(H)$ yields the following matrix equation:

$$\begin{vmatrix} \omega-\epsilon_1 & \tau & \tau & \tau & \tau & \tau & \zeta_s \\ \tau & \omega-\epsilon_2 & \tau & \tau & \tau & & \zeta_s \\ \tau & \tau & \omega-\epsilon_3 & \tau & \tau & \tau & \zeta_s \\ \tau & \tau & \tau & \omega-\epsilon_4 & \tau & \tau & \zeta_s \\ \tau & \tau & \tau & \tau & \omega-\epsilon_5 & \tau & \zeta_s \\ \tau & \tau & \tau & \tau & \tau & \omega-\epsilon_6 & \zeta_s \\ \zeta_d & \zeta_d & \zeta_d & \zeta_d & \zeta_d & \zeta_d & \omega-\epsilon_s \end{vmatrix} \cdot \begin{vmatrix} \chi_1^+ \\ \chi_2^+ \\ \chi_3^+ \\ \chi_4^+ \\ \chi_5^+ \\ \chi_6^+ \\ \chi_s^+ \end{vmatrix} = \begin{vmatrix} \eta \\ \eta \\ \eta \\ \eta \\ \eta \\ \eta \\ \eta_s \end{vmatrix} ,$$

where ($\kappa = 1, 2, \ldots, 6$)

$$\epsilon_\kappa = \gamma(H_0^z + H_\kappa^{\rm hf} + \lambda M_s^z) - \frac{i}{6}\lambda\frac{1}{T_{sd}}\chi_s - i\left(\frac{1}{T_{ds}} + \frac{1}{T_{dL}}\right) ,$$

$$\tau = \frac{i}{6}\frac{1}{T_{sd}}\lambda\chi_s ,$$

$$\zeta_s = \gamma\lambda\frac{M_d^z}{6} - \frac{i}{6}\frac{1}{T_{sd}} - \frac{i}{6}\left(\frac{1}{T_{ds}} + \frac{1}{T_{dL}}\right)\lambda\chi_d ,$$

$$\zeta_d = \gamma\lambda M_s^z - i\left(\frac{1}{T_{sd}} + \frac{1}{T_{sL}}\right)\lambda\chi_s - i\frac{1}{T_{ds}} ,$$

$$\epsilon_s = \gamma(H + \lambda M_d^z) - i\left(\frac{1}{T_{sd}} + \frac{1}{T_{sL}}\right) - i\frac{1}{T_{ds}}\lambda\chi_d ,$$

$$\eta = \frac{\gamma M_z^d}{6} + \frac{i}{6}\frac{1}{T_{sd}}\chi_s - \frac{i}{6}\left(\frac{1}{T_{ds}} + \frac{1}{T_{dL}}\right)\chi_d ,$$

$$\eta_s = \gamma M_s^z - i\left(\frac{1}{T_{sd}} + \frac{1}{T_{sL}}\right)\chi_s + \frac{1}{T_{ds}}\chi_d .$$

All the quantities are defined in the text except M_s^z and M_d^z, which are given by the "molecular field" formulas

$$M_s^z = \frac{\chi_s(1+\lambda\chi_d)}{1-\lambda^2\chi_s\chi_d}H , \quad M_d^z = \frac{\chi_d(1+\lambda\chi_s)}{1-\lambda^2\chi_s\chi_d}H .$$

APPENDIX B

The spatially dependent exchange interaction $J(R)$, neglecting enhancement, has been calculated by Davidov *et al.*[8] by taking the Fourier transform of $J(q)$. Their expression is, however, slightly in error and should be written as

$$J(R) = \frac{1}{R^4}\left\{J^{(0)}[\sin(2k_FR) - 2k_FR\cos2k_FR] + 3J^{(1)}\left[\left(2k_FR - \frac{12}{2k_FR}\right)\cos2k_FR - \left(15 - \frac{12}{(2k_FR)^2}\right)\sin(2k_FR)\right]\right.$$
$$\left. + 5J^{(2)}\left[\left(-2k_FR + \frac{84}{2k_FR} - \frac{720}{(2k_FR)^3}\right)\cos2k_FR + \left(10 - \frac{234}{(2k_FR)^2} + \frac{720}{(2k_FR)^4}\right)\sin2k_FR\right]\right\} .$$

The exchange appropriate to the long-range part, $J_{\rm eff}$(RKKY), is given by

$$J_{\rm eff}(\text{RKKY}) = (-J^{(0)} + 3J^{(1)} - 5J^{(2)}) .$$

*Supported in part by the U. S. Office of Naval Research and the National Science Foundation.
†Supported by the U. S.-Israel Binational Science Foundation and Bat-Sheva Grant for Research.
‡On leave from the Instituto de Fisica Gleb Wataghin, Universidade Estadual de Campinas, Sao Paulo, Brazil.
§Part of this work was performed at the Physics Department, University of Tel-Aviv, Israel. Support from the John Simon Guggenheim Memorial Foundation, in the form of a one-year Fellowship Grant, is very gratefully acknowledged.

[1] J. Owen, M. F. Brown, W. D. Knight, and C. Kittel, Phys. Rev. 102, 1501 (1956).
[2] A. C. Gossard, A. J. Heeger, and J. H. Wernick, J.

Appl. Phys. 38, 1251 (1967); A. C. Gossard, T. Y. Komentany, and J. H. Wernick, J. Appl. Phys. 39, 849 (1968).
[3]J. A. McElroy and A. J. Heeger, Phys. Rev. Lett. 20, 1481 (1968).
[4]K. Okuda and M. Date, J. Phys. Soc. Jpn. 27, 839 (1969).
[5]S. Schultz, M. R. Shanabarger, and P. M. Platzman, Phys. Rev. Lett. 19, 749 (1967); M. R. Shanabarger, Ph. D. thesis (University of California, San Diego, 1968) (unpublished).
[6]D. Jha and M. H. Jericho, Phys. Rev. B 3, 147 (1971).
[7]J. Kondo, in *Solid State Physics: Advances in Research and Applications*, edited by F. Seitz and D. Turnbull (Academic, New York, 1969), Vol. 23, p. 223; K. Fischer, Phys. Rev. 158, 613 (1967).
[8]D. Davidov, K. Maki, R. Orbach, C. Rettori, and E. P. Chock, Solid State Commun. 12, 621 (1973); R. E. Watson, in *Hyperfine Interactions*, edited by A. J. Freeman and R. B. Frankel (Academic, New York, 1967), p. 413.
[9]K. Mizuno, J. Phys. Soc. Jpn. 30, 742 (1971).
[10]H. Alloul (unpublished).
[11]D. C. Langreth, D. L. Cowan, and J. W. Wilkins, Solid State Commun. 6, 131 (1968).
[12]J. H. Pifer and R. T. Longo, Phys. Rev. B 4, 3797 (1971).
[13]J. Flouquet, Ann. Phys. (N.Y.) 8, 5 (1973).
[14]E. C. Hirschkoff, O. G. Symko, and J. C. Wheatley, J. Low Temp. Phys. 5, 155 (1971).
[15]J. C. Doran and O. G. Symko, Solid State Commun. 14, 719 (1974).
[16]G. Feher and A. F. Kip, Phys. Rev. 98, 377 (1955).
[17]H. Hasegawa, Prog. Theor. Phys. 21, 483 (1959).
[18]S. S. Shinozaki and A. Arrott, Phys. Rev. 152, 611 (1966).
[18a]S. Schultz and S. Oseroff (private communication).
[19]A. Narath, Phys. Rev. 163, 232 (1967).
[20]A. Narath and H. T. Weaver, Phys. Rev. 175, 373 (1968).
[21]S. Schultz, D. R. Fredkin, B. L. Gehman, and M. R. Shanabarger, Phys. Rev. Lett. 31, 1297 (1973).
[22]L. J. Tao, D. Davidov, R. Orbach, and E. P. Chock, Phys. Rev. B 4, 5 (1971).
[23]A. Blandin, J. Appl. Phys. 39, 1285 (1968); H. Alloul, J. Darville, and P. Bernier, J. Phys. F 4, 2050 (1974).
[24]L. R. Walker and R. Walstedt, Phys. Rev. B (to be published).
[25]P. Monod, Phys. Rev. Lett. 19, 1113 (1967).
[26]L. H. Bennett, R. W. Webs and R. E. Watson, Phys. Rev. 171, 611 (1968).
[27]K. Yosida, Phys. Rev. 106, 893 (1957).
[28]L. L. Hirst, Z. Phys. 245, 378 (1971).
[29]D. Davidov and D. Shaltiel, Phys. Rev. 169, 329 (1968).
[30]V. Jaccarino, in *Theory of Magnetism in Transition Metals*, edited by W. Marshall (Academic, New York, 1967), p. 335.
[31]H. Cottet, P. Donze, J. Dupraz, B. Giovanini, and M. Peter, Z. Angw. Phys. 24, 249 (1968).
[32]S. E. Barnes, J. Dupraz, and R. Orbach, J. Appl. Phys. 42, 1659 (1971), *ibid.* 42, E5908 (1971).
[33]S. E. Barnes, J. Phys. F 4, 1535 (1974).
[34]M. Peter, D. Shaltiel, J. H. Wernick, H. J. Williams, J. B. Mock, and R. C. Sherwood, Phys. Rev. 126, 1395 (1962).
[35]R. E. Walstedt and W. W. Warren, Jr., Phys. Rev. Lett. 31, 365 (1973).
[36]M.-T. Beal-Monod and R. A. Weiner, Phys. Rev. 170, 552 (1968).
[37]R. Walstedt and Y. Yafet, Solid State Commun. 11/12, 1855 (1974).
[38]H. Hundquist and P. Monod (private communication).
[39]This is found in Ref. 2 and by the present authors. The difficulty rests with the larger value of the exchange, leading to a spin-spin interaction much stronger than that for Ag:Mn. Hence, it is necessary to go to very low Mn concentrations (< 50 ppm) to be safely out of the interaction regime at He^3 temperatures. The concomitant larger thermal broadening, combined with the necessarily small Mn concentration, has so far prevented us from breaking the bottleneck sufficiently to observe the g shift.
[40]R. E. Walstedt and A. Narath, Phys. Rev. B 6, 4118 (1972).